Carcinogenesis vol.30 no.7 pp.1234–1242, 2009
doi:10.1093/carcin/bgp121
Advance Access publication May 15, 2009

Pterostilbene inhibited tumor invasion via suppressing multiple signal transduction pathways in human hepatocellular carcinoma cells

Min-Hsiung Pan*, Yi-Siou Chiou, Wei-Jen Chen[1], Ju-Ming Wang[2], Vladimir Badmaev[3] and Chi-Tang Ho[4]

Department of Seafood Science, National Kaohsiung Marine University, No. 142, Hai-Chuan Road, Nan-Tzu, Kaohsiung 811, Taiwan, [1]Department of Biomedical Sciences, Chung Shan Medical University, Taichung 402, Taiwan, [2]Institute of Biosignal Transduction, College of Bioscience and Biotechnology, National Cheng Kung University, Tainan 701, Taiwan, [3]Sabinsa Corporation, 70 Ethel Road West Unit 6, Piscataway, NJ 08854, USA and [4]Department of Food Science, Cook College, Rutgers University, New Brunswick, NJ 08901-8520, USA

*To whom correspondence should be addressed. Tel: +886 7 361 7141; Fax: +886 7 361 1261;
Email: mhpan@mail.nkmu.edu.tw

Pterostilbene, a natural dimethylated analog of resveratrol, is known to have diverse pharmacologic activities including anticancer, anti-inflammation, antioxidant, apoptosis, anti-proliferation and analgesic potential. However, the effects of pterostilbene in preventing invasion of cancer cells have not been studied. Here, we report our finding that pterostilbene significantly suppressed 12-*O*-tetradecanoylphorbol 13-acetate (TPA)-induced invasion, migration and metastasis of human hepatoma cells ($HepG_2$ cells). Increase in the enzyme activity, protein and messenger RNA levels of matrix metalloproteinase (MMP)-9 were observed in TPA-treated $HepG_2$ cells, and these were blocked by pterostilbene. In addition, pterostilbene can inhibit TPA-induced expression of vascular endothelial growth factor, epidermal growth factor and epidermal growth factor receptor. Transient transfection experiments also showed that pterostilbene strongly inhibited TPA-stimulated nuclear factor kappa B (NF-κB) and activator protein-1 (AP-1)-dependent transcriptional activity in $HepG_2$ cells. Moreover, pterostilbene can suppress TPA-induced activation of extracellular signal-regulated kinase 1/2, p38 mitogen-activated protein kinase, c-Jun N-terminal kinases 1/2 and phosphatidylinositol 3-kinase/Akt and protein kinase C that are upstream of NF-κB and AP-1. Significant therapeutic effects were further demonstrated *in vivo* by treating nude mice with pterostilbene (50 and 250 mg/kg intraperitoneally) after inoculation with $HepG_2$ cells into the tail vein. Presented data reveal that pterostilbene is a novel, effective, anti-metastatic agent that functions by down-regulating MMP-9 gene expression.

Introduction

Pterostilbene (*trans*-3,5-dimethoxy-4′-hydroxystilbene), a natural dimethylated analog of resveratrol from blueberries, is known to have diverse pharmacologic activities including anticancer, anti-inflammation, antioxidant, antiproliferatory and analgesic activity (1). Our previous studies reported that pterostilbene has the ability to inhibit lipopolysaccharide-induced inflammation in mouse macrophages (2). Although various bioactivity studies of pterostilbene have been carried out, studies regarding the molecular mechanisms by which pterostilbene acts on the expression of matrix metalloproteinase (MMP)-9 and the invasiveness of $HepG_2$ are still undefined.

Invasion and metastasis are fundamental properties of malignant cancer cells. Hepatocellular carcinoma is the most common malignant tumor in the liver, and the prognosis of patients with this type of cancer is primarily determined by the incidence of recurrence after surgery and the occurrence of invading metastases into the remaining liver parenchyma (3,4). The formation of metastatic nodules of hepatocellular carcinoma involves an intricate multiprocessing cascade, including cell adhesion, migration and proteolysis of the extracellular matrix. Among these enzymes, the MMPs, which are a family of zinc-dependent endopeptidases, are deeply involved in the invasion and metastasis of various tumor cells (5–7).

MMPs can be divided into four subclasses based on their substrate. These are collagenase, gelatinase, stromelysin and membrane-associated MMPs (8). To date, 24 kinds of MMPs have been identified, and MMP-2 (gelatinase-A) and MMP-9 (gelatinase-B) are most associated with tumor migration, invasion and metastasis for various human cancers (9–11). Tumor-secreted MMPs destroy extracellular matrix components in tissue surrounding a tumor, enter and survive in the circulation, lymphatics or peritoneal spaces and can arrest in a distant target organ. Generally, MMP-2 is constitutive and overexpressed in highly metastatic tumors, whereas MMP-9 can be stimulated by an inflammatory cytokine (e.g. tumor necrosis factor-α) (12), a growth factor (e.g. vascular endothelial growth factor (VEGF), epidermal growth factor (EGF) and transforming growth factor-β) (13–15) or an oncogene (e.g. Ras) (16–18) through activation of different intracellular-signaling pathways. Among these stimulators, 12-*O*-tetradecanoylphorbol 13-acetate (TPA) is a well-known substitute for diacylglycerol as a high affinity ligand for conventional protein kinase C and novel protein kinase C (PKC) isoforms (19). Activation of PKC results in translocation of the protein to membranes and controls the expression of MMP-9 by modulating the activation of transcription factors including activator protein-1 (AP-1), nuclear factor kappa B (NF-κB) or specificity protein 1 through mitogen-activated protein kinase (MAPK)-signaling pathway and phosphatidylinositol 3-kinase(PI3K)-signaling pathway (20–23). Several studies indicate that inhibition of MMP expressions or enzyme activities can be used as early targets for preventing cancer metastasis (24–26). Therefore, agents possessing the ability to suppress the expression of MMP-2 or -9 are worthy of development for anti-hepatoma cancer invasion and metastasis.

In this research, we first studied the effect of pterostilbene on TPA-induced MMPs expression and explored the underlying upstream signaling molecular mechanisms. We also tested the anti-metastasis of pterostilbene in mouse model. Pterostilbene significantly suppressed MMP-9 gene expression via blocking the conventional protein kinase C-/MAPK-, PI3K/NF-κB- and AP-1-signaling pathways and consequently reduced invasion and metastasis of $HepG_2$ cells.

Materials and methods

Reagents

TPA was purchased from Sigma Chemical Co. (St Louis, MO). All other chemicals used were in the purest form available commercially. PD98059 [an extracellular signal-regulated kinase (ERK) inhibitor], SB202190 (a p38 MAPK inhibitor), SP600125 [a c-Jun N-terminal kinase (JNK) inhibitor], LY294002 (an Akt inhibitor) and GF109203XP (a PKC inhibitor) were purchased from Calbiochem (EMD Chemical, San Diego, CA). Pterostilbene was synthesized according to the method reported by Pettit *et al.* (27). The purity of pterostilbene was determined by high-performance liquid chromatography (HPLC) as >99.2%.

Cell culture

$HepG_2$ cells were grown in Dulbecco's modified Eagle's medium (DMEM) containing 10% fetal bovine serum, 100 μg/ml streptomycin and 100 U/ml penicillin in a humidified atmosphere containing 5% CO_2 at 37°C. In the

Abbreviations: AP-1, activator protien-1; DMEM, Dulbecco's modified Eagle's medium; EGF, epidermal growth factor; EMT, epithelial–mesenchymal transition; ERK, extracellular signal-regulated kinase; HPLC, high-performance liquid chromatography; JNK, c-Jun N-terminal kinase; MAPK, mitogen-activated protein kinase; MET, mesenchymal–epithelial transition; MMP, matrix metalloproteinase; NF-κB, nuclear factor-kappa B; PCR, polymerase chain reaction; PI3K, phosphatidylinositol 3-kinase; PKC, protein kinase C; TPA, 12-O-tetradecanoylphorbol 13-acetate; VEGF, vascular endothelial growth factor.

invasion and metastasis experiments, the cells were cultured in a serum-free medium.

3-(4,5-Dimethylthiazole-2-yl)-2,5-biphenyl tetrazolium bromide assay

$HepG_2$ cells were subcultured into 96-well culture plates at a density of 10^5 per well in 100 µl of DMEM medium. The next day, the medium was changed and various concentrations of pterostilbene were added. Control cells were treated with dimethyl sulfoxide to yield a final concentration of 0.05% (vol/vol). After 12 h of incubation, the medium was discarded and cells were washed with phosphate-buffered saline. A 100 µl of 3-(4,5-dimethylthiazole-2-yl)-2,5-biphenyl tetrazolium bromide was added to each well, and the plates were incubated at 37°C for 4 h. Then, 100 µl of dimethyl sulfoxide was added to each well and we determined the absorbance of the oxidized 3-(4,5-dimethylthiazole-2-yl)-2,5-biphenyl tetrazolium bromide solution at 570 nm by an enzyme-linked immunosorbent assay reader. All experiments were performed in triplicate.

Wound-healing assay

$HepG_2$ cells were grown to 90% confluence in a 6-well plate at 37°C, 5% CO_2 incubator. A wound was created by scratching cells with a sterile 200 µl pipette tip, cells were washed twice with phosphate-buffered saline to remove floating cells and then added to a medium without serum. Photos of the wound were taken under ×100 magnitude microscope.

Soft agar colony formation assay

Culture dishes (6 cm) were covered with a layer (7 ml) of 0.7% agarose in a medium supplemented with 20% fetal bovine serum. Cell suspensions (5×10^4 per dish) were prepared in 1 ml of 0.35% agar and poured into the dishes. The dishes were cultured at 37°C, 5% CO_2, incubated for 20 days and then photographed using a light microscope. The numbers of colonies with diameters >0.3 mm were counted. Each value is derived from three independent experiments and results are expressed as the mean ± SE.

Cell adhesion assay

$HepG_2$ cells were released from the culture dishes with trypsin. Cells suspended (5×10^4/2 ml) in DMEM were applied to a 6-well plate and incubated for 2 h. Cell adhesion was monitored by photographing under ×200 magnitude.

Invasion assay

Matrigel-coated filter inserts (8 µm pore size) that fit into 24-well invasion chambers were obtained from Becton Dickinson (Franklin Lakes, NJ). $HepG_2$ cells to be tested for invasion were detached from the tissue culture plates and resuspended in serum DMEM medium (5×10^4 cells/200 µl), with the presence or absence of drugs (TPA and pterostilbene), and then added to the upper side of the invasion chamber. Serum-containing DMEM medium (500 µl) was added to the lower chamber. After 24 h of incubation, filter inserts were removed from the wells and the cells on the upper surface of the filter were removed using cotton swabs. The cells on the lower surface were fixed with 4% formaldehyde, stained (0.1% crystal violet in 20% ethanol) and then counted. Cell invasion was monitored by photographing under ×400 magnitude.

Gelatin zymography

$HepG_2$ cells were incubated in serum-free DMEM in the presence of 200 nM TPA with or without pterostilbene for the indicated time; the conditioned medium was then collected as samples. The unboiled samples (medium or serum from nude mice) were separated by electrophoresis on 10% sodium dodecyl sulfate–polyacrylamide gel electrophoresis containing 0.1% gelatin. After electrophoresis, gels were soaked in 2.5% Triton X-100 in dH_2O (2×30 min) at room temperature and then incubated in substrate buffer (50 mM Tris–HCl, 5 mM $CaCl_2$, 0.02% NaN_3 and 1% Triton X-100, pH 8.0) at 37°C for 18 h. Bands corresponding to activity were visualized by negative staining using 0.3% Coomassie blue in 50% methanol and 10% acetic acid.

Western blotting

The samples (50 µg of protein) of total cell lysates or cytosolic and membrane fractions were size fractionated by sodium dodecyl sulfate–polyacrylamide gel electrophoresis and electrophoretically transferred onto a polyvinylidene difluoride membrane (Millipore Corporation, Bedford, MA). The membranes were blocked using a blocking solution (20 mM Tris–HCl, pH 7.4; 0.2% Tween 20; 1% bovine serum albumin and 0.1% sodium azide). The membrane was then further incubated with specific antibodies, at appropriate dilutions, using blocking solutions such as anti-ERK, anti-p38, anti-JNK, anti-PI3K, anti-Akt, anti-VEGF, anti-epidermal growth factor receptor (membrane and total), anti-conventional protein kinase C (cytosolic and membrane), anti-EGF and anti-MMP-9 overnight at 4°C. Then, the membranes were subsequently probed with anti-mouse, anti-rabbit or anti-goat IgG antibody, conjugated with horseradish peroxidase (Transduction Laboratories, Lexington, KY) and detection was achieved by measuring the chemiluminescence of the blotting agent (enhanced chemiluminescence, Amersham Corporation, Arlington Heights, IL) after exposure of the filters on Kodak X-Omat films. The densities of the bands were quantitated with a computerized densitometer (AlphaImager™ 2200 System). The total proteins were extracted via the addition of 200 µl of gold lysis buffer (50 mM Tris–HCl, pH 7.4; 1 mM NaF; 150 mM NaCl; 1 mM ethyleneglycol-bis(aminoethylether)-tetraacetic acid; 1 mM phenylmethylsulfonyl fluoride; 1% nonidet P-40 and 10 mg/ml leupeptin) to the cell pellets on ice for 30 min, followed by centrifugation at 12 000*g* for 30 min at 4°C. The cytosolic fractions were extracted via the addition 100 µl of hypotonic buffer (50 mM NaCl, 0.3 mM Na-orthovanadate, 50 mM NaF, 10 µg/ml leupeptin and 5 µg/ml aprotinin) on ice for 30 min, followed for overnight at −80°C. They were ice-out at room temperature, recycled thrice and then centrifuged at 12 000*g* for 2 h at 4°C. The pellets were added to 100 µl lysis buffer (25 mM Tris base, 250 mM NaCl, 2 mM ethylenediaminetetraacetic acid, 1% nonidet P-40, 0.1 mM phenylmethylsulfonyl fluoride, 50 µg/ml leupeptin and 50 µg/ml aprotinin) on ice for 30 min, followed by centrifugation at 12 000*g* for 2 h at 4°C.

Reverse transcription–polymerase chain reaction

Total RNA was prepared from $HepG_2$ cells using TRIZOL reagent according to supplier's protocol. The template used was 4 µg total cellular RNA in a 20 µl reaction solution with Super Script II RNAse H-reverse transcriptase (Invitrogen, Renfrewshire, UK). The complementary DNA (2 µl) was amplified by polymerase chain reaction (PCR) with the following primers: MMP-9 (480 bp) 5′-CAACATCACCTATTGGATCC-3′ (sense), 5′-CTGTAGAGTCTCTC-GCT-3′ (anti-sense); β-actin (298 bp) 5′-AAGAGAGGCATCCTCACCCT-3′ (sense) and 5′-TACATGGCTGGGGTGTTGAA-3′ (anti-sense). PCR amplification was performed under the following conditions: 30 cycles at 94°C for 1 min, 50°C for 1 min, 72°C for 2 min and followed by a final incubation at 72°C for 10 min. PCR products were analyzed by 1% agarose gel and visualized by ethidium bromide staining.

Transient transfection and luciferase assay

The luciferase assay was performed as described by George *et al.* (28) with some modifications. $HepG_2$ cells were seeded in a 60 mm dish. When the cells reached confluence, the medium was replaced with serum-free Opti-MEM (Gibco BRL, Grand Island, NY). The human MMP-9 promoter fragment from −1940 to +113 bp (hMMP-9 −1940/+113) was obtained by genomic PCR. The primers used were as follows: MMP9/KpnI-1940: 5′-GGGGTACCAGTGACTTGCC-CAAGGTCACATAGC-3′ and MMP9/HindIII+113: 5′-CCCAAGCTTTGA-GATTGGTTCTCAGGTCTCCAGG-3′. The KpnI/HindIII fragment was subcloned into the plasmid of gene light 2-basic vector (Promega Corporation, Madison, WI) and verified by sequencing. The cells were then transfected with the hMMP-9 promoter, pNF-κB-Luc and pAP-1-Luc plasmid reporter gene (Stratagene, La Jolla, CA) using LipofectAMINE™ reagent (Invitrogene™, Carlsbad, CA). After 24 h of incubation, the medium above was replaced with complete medium. After another 24 h, the cells were trypsinized and equal numbers of cells were plated in 12-well tissue culture plates for 18 h. The cells were then incubated with 200 nM TPA and pterostilbene for 12 h. Each well was then washed twice with cold phosphate-buffered saline and harvested in 150 µl of lysis buffer (0.5 M *N*-2-hydroxyethylpiperazine-*N*′-2-ethanesulfonic acid, pH 7.8; 1% Triton N-101; 1 mM $CaCl_2$ and 1 mM $MgCl_2$). Luciferase activity was assayed by means of the LucLite™ luciferase reporter gene kit (Packard BioScience Company, Meriden, CT), with 100 µl of cell lysate used in each assay. Luminescence was measured on a Top Counter Microplate Scintillation and Luminescence Counter (Packard 9912 V) in single-photon counting mode for 0.1 min per well, following a 5 min adaptation in the dark. Luciferase activities were determined and normalized to protein concentrations.

PKC activity assay

Membrane fractions from $HepG_2$ cells were extracted in order to determine the effect of TPA-induced and pterostilbene inhibition on PKC activity. The PKC activity in the membrane fraction was tested using an Assay Designs non-radioactive PKC activity enzyme-linked immunosorbent assay kit (Assay Designs, Stressgen, Ann Arbor, MI), according to the manufacturer's instructions. Final color development is halted with an acid stop solution and the intensity of the color measured by absorbance at 450 nm.

Direct MMP-9 enzyme activity assay

Conditioned medium derived from TPA-treated $HepG_2$ cells was incubated with 10, 25 and 50 µM pterostilbene at 37°C 30 min, respectively. Twenty microliters of incubated buffer was analyzed for gelatinolytic activity as described as above.

Experimental pulmonary metastasis

Five-week-old male nude mice (purchased from the BioLASCO Experimental Animal Center, Taiwan Co., Ltd, Taipei, Taiwan) were maintained in

pathogen-free sterile isolators according to institutional guidelines and all food, water, caging and bedding were sterilized before use. All procedures were approved by the National Animal Care and Use Committee. To assess the efficacy of pterostilbene against tumor metastasis, $HepG_2$ cells (1×10^6/200 μl) were injected into male nu/nu mice via tail vein to imitate tumor metastasis. To evaluate the effect of pterostilbene on lung metastasis, experimental animals received either 20 μl intraperitoneal injections of corn oil (control group) or pterostilbene (50 and 250 mg/kg) five times per week (active group) beginning on the day of tumor cell implantation. The mice were killed 10 weeks after the inoculation and lungs were removed and fixed in formaldehyde. The number of surface foci was determined.

Plasma sample preparation

Pterostilbene was given intraperitoneally at a dose of 50 or 250 mg/kg, respectively, and the mice were killed at 30 min and 24 h after administration. Plasma was obtained from blood (treated with 0.2 mg/ml heparin) by centrifugation at 4300*g* for 10 min, subsequently acidified to pH 3.0 with 6 N HCl and extracted two times with equal volumes of ethyl acetate:propanol (9:1, vol/vol). The extraction recovery from plasma was ∼95%. The plasma samples were separated by centrifugation at 5000*g* for 10 min in a desktop centrifuge and filtered through 0.22 μM polyvinylidene difluoride membrane filters. Sample detection was achieved at 330 nm and injection volumes were 20 μl.

HPLC system and condition

HPLC was performed with a system with Hitachi HPLC (Kyoto, Japan), a ultraviolet detector, and a Waters Nova-Pak C_{18} column (150 × 3.9 mm, 5 μm particle size) was used. The mobile phase consisted of methanol and HPLC water (50:50 vol/vol) that was filtered and degassed under reduced pressure prior to use. Separation was carried out isocratically at ambient temperature and a flow rate of 1 ml/min. Sample detection was achieved at 330 nm, and injection volumes were 20 μl. Chromatographic peaks of incubation samples were identified by spiking with chromatographic authentic standards.

Statistical analysis

Data are presented as mean ± SE for the indicated number of independently performed experiments. A one-way Student's *t*-test was used to assess the statistical significance between the TPA and the pterostilbene plus TPA-treated groups. A *P*-value of <0.05 was considered statistically significant.

Results

Pterostilbene inhibited TPA-induced invasion, colony formation and migration in human hepatoma cells

In vitro invasion and migration assays including transwell, soft agar and wound healing were used to investigate the inhibitory effect of pterostilbene on the invasive potency of human hepatoma $HepG_2$ cells. As illustrated in Figure 1A, the cytotoxicity of TPA and pterostilbene was evaluated by 3-(4,5-dimethylthiazole-2-yl)-2,5-biphenyl tetrazolium bromide assay and microscopy examination. It is apparent that there were no cytotoxic effects of pterostilbene at 50 μM in $HepG_2$ and at 25–100 μM in human lymphocyte cells (Figure 1B). TPA induction of invasion and colony formation was detected by transwell and soft agar assays, and the treatment of pterostilbene significantly inhibited its induction (Figure 1C and E). Quantitative data derived from three independent experiments supported pterostilbene effectively inhibited the invasion (Figure 1D) and colony formation (Figure 1F) of $HepG_2$ cells elicited by TPA. Because epithelial–mesenchymal transition (EMT) and mesenchymal–epithelial transition (MET) are commonly

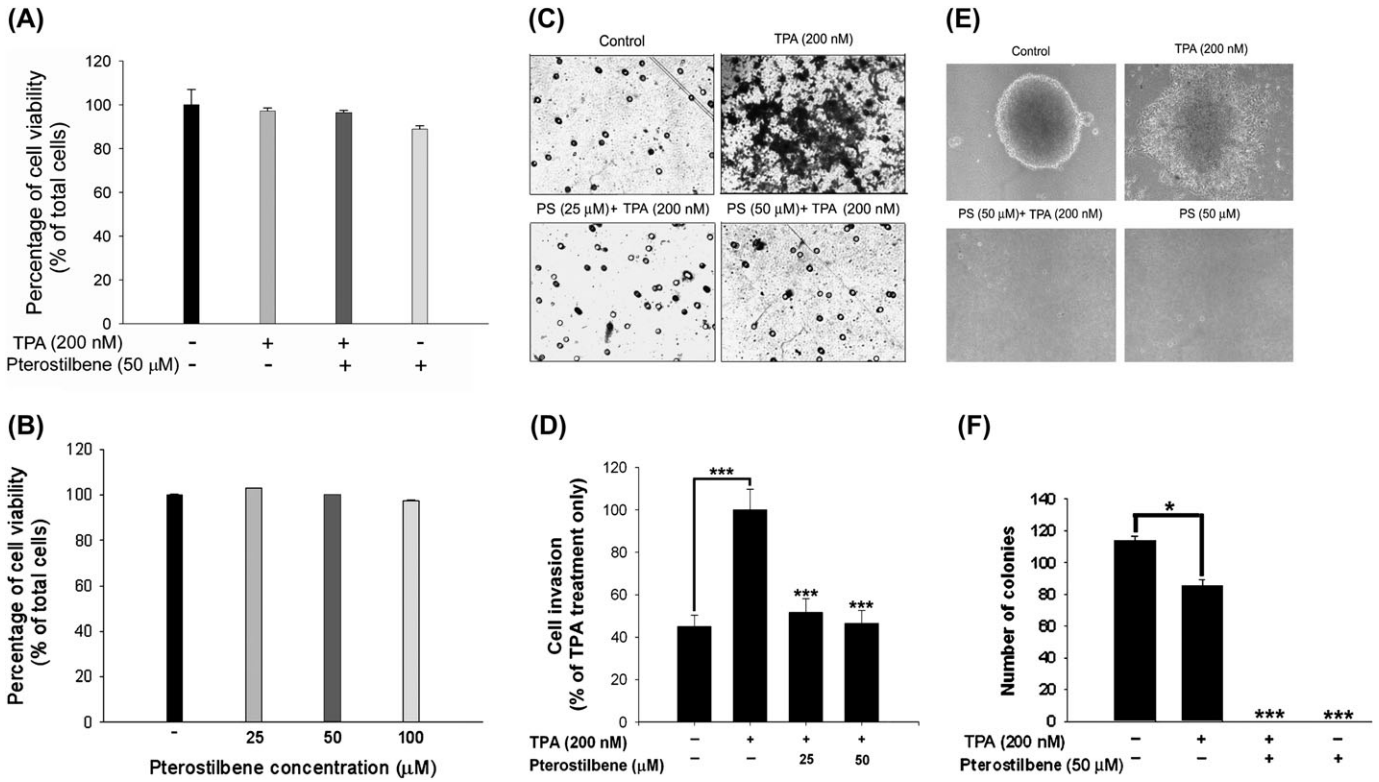

Fig. 1. Effects of pterostilbene (PS) on TPA-induced cell invasion and transformation. (**A**) $HepG_2$ cells were treated with TPA, PS and PS/TPA for 12 h. (**B**) Human lymphocyte cells were treated with 25–100 μM of the indicated PS for 12 h. Cell viability was determined by 3-(4,5-dimethylthiazole-2-yl)-2,5-biphenyl tetrazolium bromide assay. The percentage of cell viability was calculated as the ratio (A_{570}) of treated cells to control cells. Data represent the ± SE of three independent experiments. (**C**) $HepG_2$ cells were treated with various dose of PS (0, 25 and 50 μM) for 24 h in the presence of 200 nM TPA. Cells in the lower chamber were then stained and quantified (**D**) as described in the text. A representative number of invading cells through the Matrigel were counted under the microscope in three random fields at a ×400 magnification. Each bar represents the mean ± SE of the averages of triplicate plates and three fields counted. Results were statistically analyzed with Student's *t*-test ($^{***}P < 0.001$ compared with the TPA treatment only). (**E**) $HepG_2$ cells (5×10^4) were treated with TPA, PS/TPA and PS in soft agar for 20 days. Microphotographs showed morphologic alteration in soft agar colony formation assay. Photos of the colonies were taken under ×100 magnitude microscope. (**F**) The number of colonies in soft agar was counted. The number of colonies with diameter >0.3 mm were apparent in dishes containing $HepG_2$ cells. The results shown are the means ± SEs of the averages of triplicate plates and are representative of three independent experiments. Results were statistically analyzed with Student's *t*-test ($^{*}P < 0.05$ and $^{***}P < 0.001$ compared with the TPA treatment only).

associated with acquisition of metastatic potential, we investigated whether pterostilbene suppressed TPA-induced EMT–MET. Strikingly, it is apparent that TPA induced EMT. Thus, TPA-treated cells exhibited a more motile, spindle-like morphology with a loss of cell–cell contact, whereas pterostilbene treatment maintained a typical spreading epithelial cell phenotype (Figure 2A). We also assessed the effect of pterostilbene-inhibited TPA-induced cell MET processes. As shown in Figure 2B, 2 h after plating the cells in fresh culture dishes, the majority of TPA-treated cells displayed a adhesion/spreading morphology and were inhibited by adding pterostilbene. To determine whether pterostilbene also inhibited TPA-induced migration on the surface of the tissue culture plate, we performed wound-healing experiments. As shown in Figure 2C, migration of $HepG_2$ cells was increased by TPA incubation and inhibited by treatment with pterostilbene (Figure 2C). Taken together, the results show that pterostilbene inhibited TPA-induced cell motility, transformation and EMT–MET, which the acquisition of invasive properties is consistent with tumor metastasis.

Pterostilbene inhibited TPA-induced MMP-9 enzyme activity via reducing its gene and protein levels

We examined the effect of pterostilbene on MMP-9 activity, which is related to the invasion and metastasis of hepatocellular carcinoma as evidenced by gelatin zymography. As shown in Figure 3A, MMP-9 activity was strongly induced by TPA at 12 h and pterostilbene dramatically inhibited the proteolytic activity of MMP-9 in a dose-dependent manner (Figure 3B). We studied the effect of pterostilbene on the levels of MMP-9 messenger RNA in $HepG_2$ cells stimulated by TPA. Treatment of $HepG_2$ with pterostilbene, in the presence of TPA, induced a decrease in the levels of MMP-9 messenger RNA, as evidenced by reverse transcription–PCR analysis (Figure 3C). In addition, pterostilbene blocked TPA-induced MMP-9 expression as evidenced by western blot analysis (Figure 3D). Moreover, as shown in Figure 3D, pterostilbene dramatically inhibited TPA-induced VEGF, EGF and epidermal growth factor receptor expression in $HepG_2$ cells. These results show that pterostilbene inhibits the transcriptional activity of MMP-9 in TPA-induced human hepatoma cells. To investigate if pterostilbene reduces MMP-9 enzyme activity through the direct inhibition of the MMP-9 enzyme, incubation of pterostilbene with conditioned medium derived from TPA-treated $HepG_2$ cells followed by gelatin zymography analysis was performed. As shown in Figure 3E, there was no significant difference between the groups with or without pterostilbene treatment.

Inhibition of transcriptional activity of MMP-9 gene through suppression of TPA-induced NF-κB and AP-1 activity by pterostilbene

To investigate the importance of TPA and pterostilbene in modulating expression of MMP-9, transient transfections were performed using human MMP-9 luciferase promoter constructs. Treatment with TPA led to an ∼6.5-fold increase in MMP-9 promoter activities that was inhibited by pterostilbene in a dose-dependent manner (Figure 4A). The MMP-9 promoter contains two important transcriptional elements, namely the binding sites of NF-κB and AP-1. To further investigate whether pterostilbene modulates MMP-9 expression through the inhibition of TPA-stimulated NF-κB and AP-1 activity, the pNF-κB-Leu and pAP-1-Leu reporter plasmids were cotransfected with pGFPemd-cmv control plasmids into $HepG_2$ cells. Pterostilbene significantly inhibited TPA-induced NF-κB and AP-1 transcriptional activity in a dose-dependent manner (Figure 4B and C). These results clearly show that pterostilbene regulated the transcriptional activation of MMP-9 through the inhibition of TPA-stimulated NF-κB and AP-1 activity.

Inhibitory effect of pterostilbene on TPA-induced activation of MAPKs, PI3K and Akt/protein kinase B

MAPKs are known to regulate NF-κB activation by multiple mechanisms. Studies show that the p38-, ERK- and PI3K/Akt-signaling pathways are involved in TPA-mediated induction of MMP-9 (29,30), occurs through diverse mechanisms; however, studies regarding these mechanism of pterostilbene's downregulation of MMP-9 through

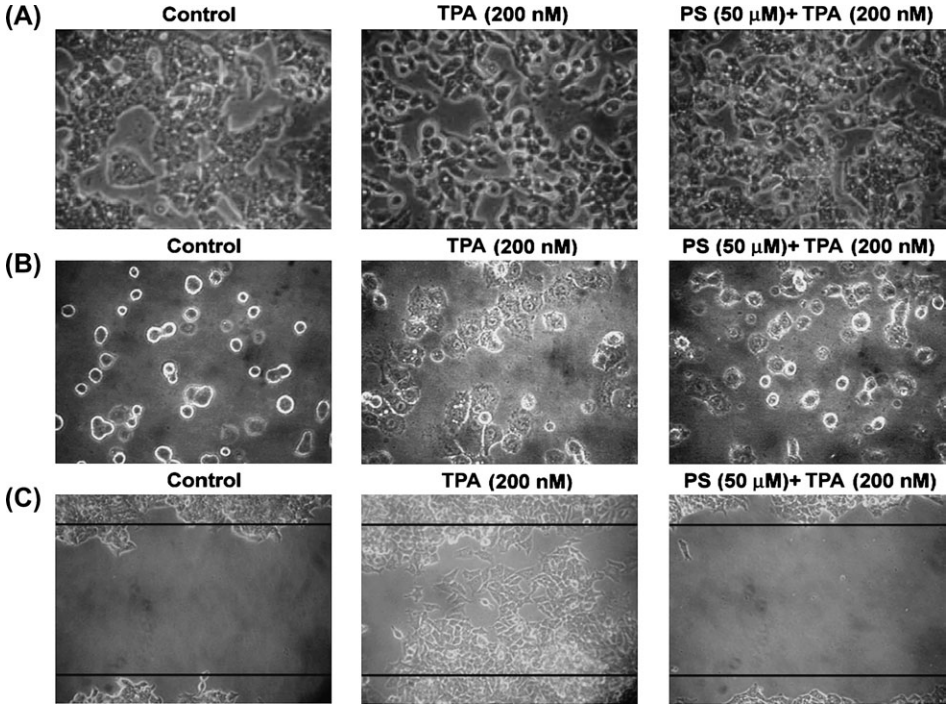

Fig. 2. Effects of pterostilbene (PS) on TPA-induced EMT, adhesion/spreading and wound healing of $HepG_2$ cells. (**A**) Cells were treated with TPA and PS/TPA for 12 h and then cell morphological characteristics were examined by light microscopic in random fields at a ×100 magnification. (**B**) $HepG_2$ cells were treated with TPA and PS/TPA in 2 ml of DMEM and applied to a six-well plate and incubated for 2 h. Cell adhesion was monitored by photographing under ×200 magnitude. (**C**) Cells were treated with TPA and PS/TPA in six-well plate and incubated for 24 h. Photos of the wound were taken under ×100 magnitude microscope.

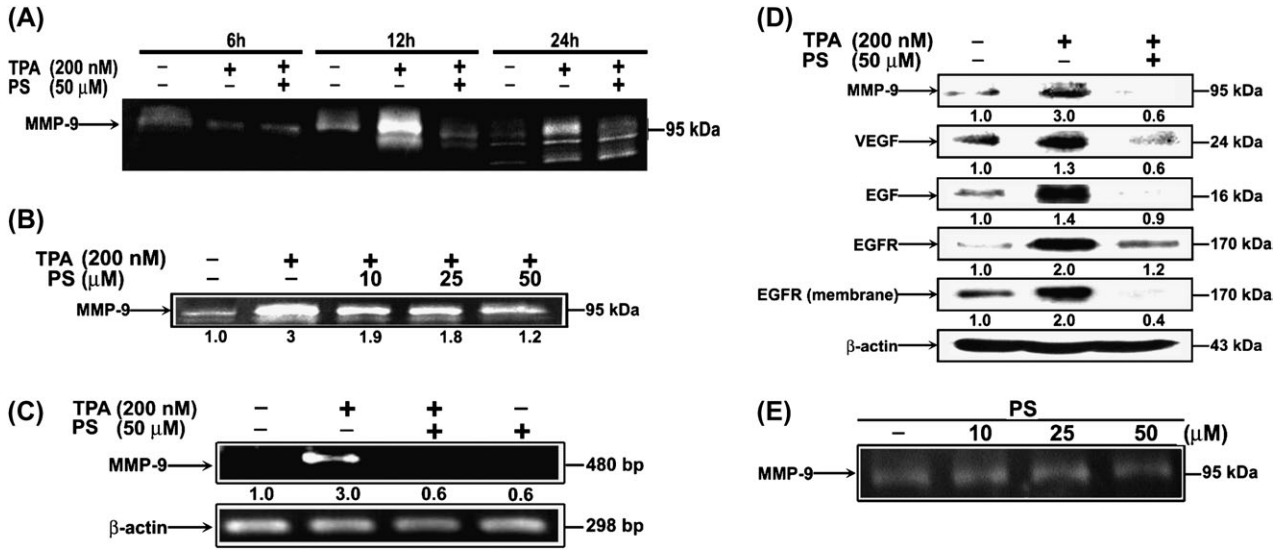

Fig. 3. Inhibitory effects of pterostilbene (PS) on TPA-induced MMP-9 activity, MMP-9 messenger RNA expression and metastatic-related protein expression of $HepG_2$ cells. (**A**) Time course and (**B**) concentration-dependent inhibitory effects of PS on TPA-induced MMP-9 activity. $HepG_2$ cells were grown for the indicated periods in serum-free medium. Conditioned media were subjected to 10% sodium dodecyl sulfate–polyacrylamide gel electrophoresis with 0.1% gelatin and the gelatinolytic activities of MMP-9 and MMP-2 were determined by gelatin zymography as described in Materials and Methods. The values under each lane indicate relative density of the band compared with control. (**C**) The RNA extracted from $HepG_2$ cells was subjected to a RT–PCR. β-Actin was used as internal control. (**D**) $HepG_2$ cells were cultured in serum-free media containing 200 nM TPA and 50 μM PS for 12 h and then the cell lysates were subjected to sodium dodecyl sulfate–polyacrylamide gel electrophoresis followed by western blots as described in Material and Methods. The values under each lane indicate relative density of the band normalized to β-actin. (**E**) MMP-9 derived from TPA-treated conditioned medium were incubated with PS (10, 25 and 50 μM) for 30 min and then subjected to gelatin zymography. All analyses were representative of at least three independent experiments.

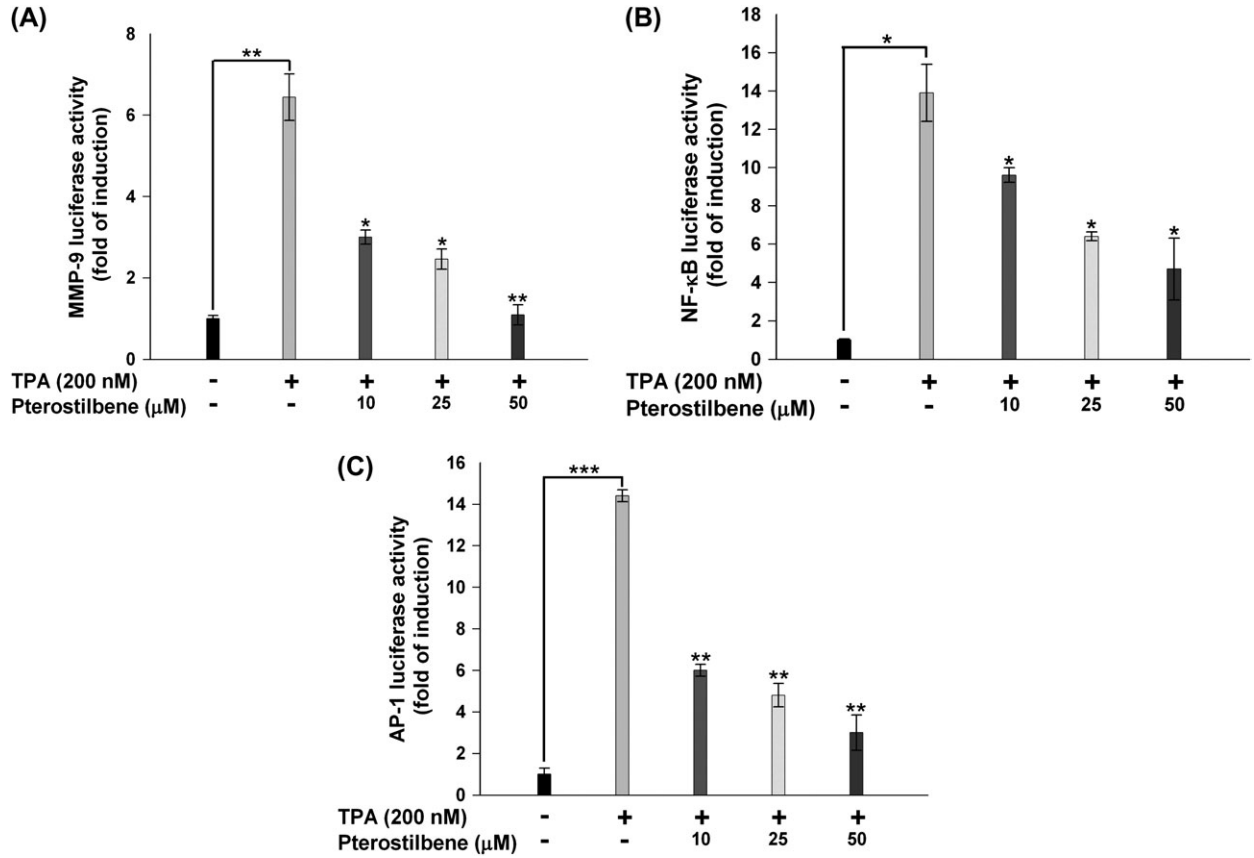

Fig. 4. Inhibitory effects of pterostilbene on NF-κB- and AP-1 DNA-binding activities. The cells were transiently transfected with 2.5 μg of (**A**) hMMP-9 promoter (**B**) pNF-κB-Luc and (**C**) pAP-1-Luc reporter plasmid and then treated with pterostilbene at a dose of 0, 10, 25 and 50 μM in the presence of TPA (200 nM) for 12 h. Then cellular protein was extracted for measuring luciferase activity assay. Each bar represents the mean ± SE of the averages of triplicate experiments. Results were statistically analyzed with Student's *t*-test ($^{*}P < 0.05$, $^{**}P < 0.01$ and $^{***}P < 0.001$ indicate statistically significant differences from the TPA-treated group).

suppression of MAPK or PI3K have not been carried out. Therefore, we investigated the effects of pterostilbene on TPA-induced phosphorylation of ERK, p38, JNK and PI3K/Akt activity in $HepG_2$ cells. Western blot analysis revealed that TPA alone caused significant increase in the phosphorylation of ERK, p38, JNK, PI3K and Akt as compared with vehicle-treated controls, and these were blocked by pretreatment with pterostilbene (Figure 5A–C). More importantly, no change was observed in the total MAPK and PI3K/Akt content in cells treated with both TPA and pterostilbene. Pharmacological inhibitors of MAPK and PI3K/Akt including PD98059 (an ERK inhibitor), SB202190 (a p38 MAPK inhibitor), SP600125 (a JNK inhibitor) and LY294002 (an Akt inhibitor) were used to identify the molecular signaling pathways by which TPA stimulates MMP-9 expression. As illustrated in Figure 5D, treatment of cells with these inhibitors markedly abrogated TPA-induced MMP-9 enzyme activity.

Pterostilbene suppresses PKC activation elicited by TPA

Previous studies demonstrated that PKC acts as the major receptor in response to TPA *in vitro* and *in vivo* and also plays an important role in transmembrane signal transduction (31). Activation of PKCs has been correlated with the potential of tumor metastasis (32). In the present study, we also demonstrated that pretreatment with pterostilbene significantly reduced TPA-induced translocation of PKCα, β and γ protein from cytosol to the membrane (Figure 6A) and PKCs activity (Figure 6B) in $HepG_2$ cells. To identify the molecular mechanism, pharmacological experiments using PKC inhibitor (GF109203X) were performed in the present study. As shown in Figure 6C, incubation of $HepG_2$ cells with GF109203X inhibited TPA-induced MMP-9 enzyme activity. Data from the Matrigel invasion assay revealed that the incubation with GF109203X and PD98059 significantly inhibited TPA-induced invasion of $HepG_2$ cells (Figure 6D). Thus, it is possible that pterostilbene can affect the activity of PKC as well as further downstream signaling, which is involved in TPA-stimulated MMP-9 activation and invasion.

Inhibitory effect of pterostilbene on metastasis to lung

We further examined the therapeutic efficacy of pterostilbene against tumor metastasis, $HepG_2$ cells were injected into nude mice *via* tail

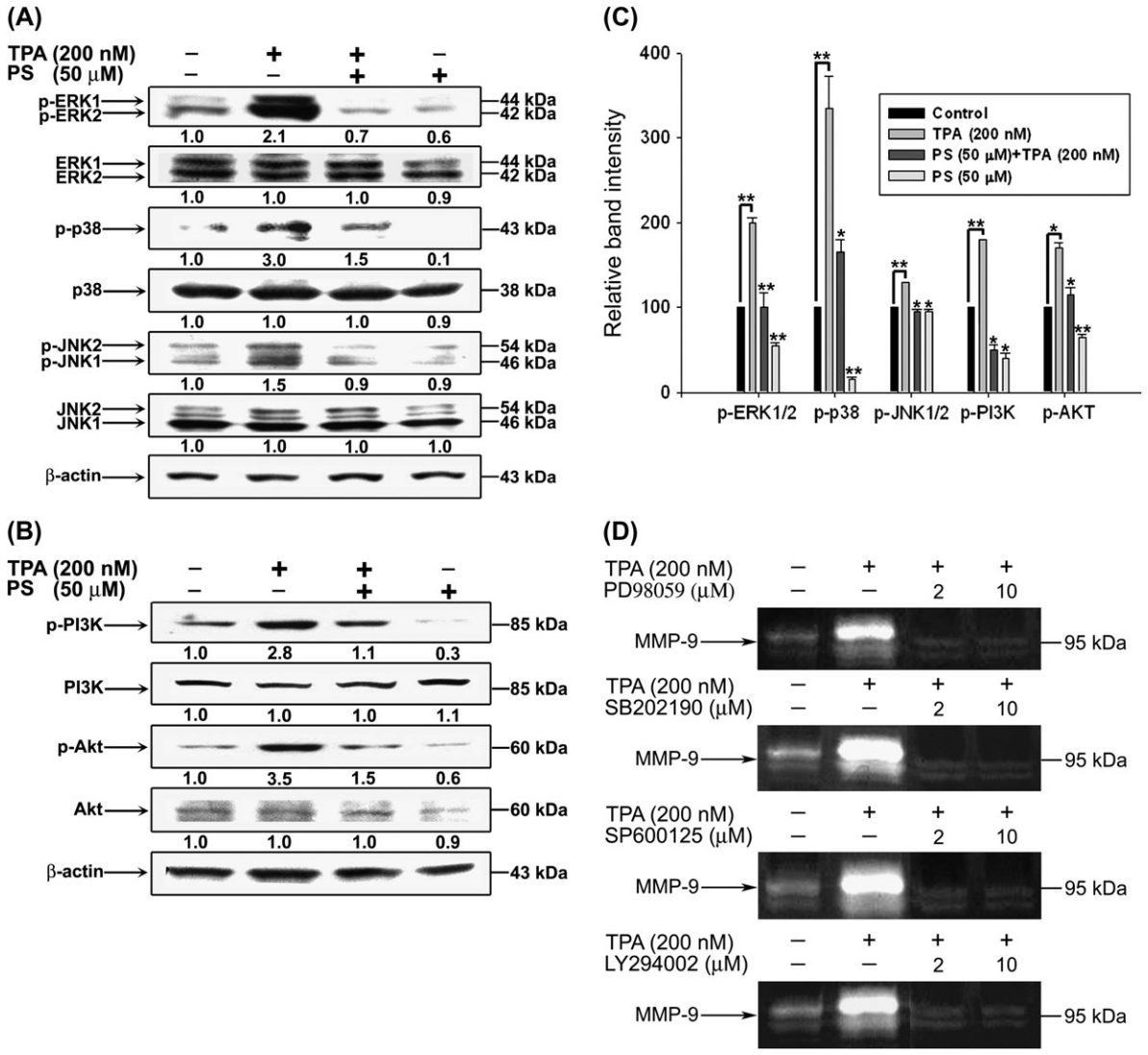

Fig. 5. Effects of pterostilbene (PS) on TPA-induced activation of MAPK and PI3K/Akt signalings. (**A** and **B**) $HepG_2$ cells were cultured in serum-free media containing TPA, PS and PS/TPA for 12 h and then the cell lysates were subjected to sodium dodecyl sulfate–polyacrylamide gel electrophoresis followed by western blots as described in Materials and Methods. Each bar represents the mean ± SE of the averages of three independent experiments. (**C**) Quantification of phospho-MAPKs and phosphor-PI3K/Akt proteins was performed by densitometric analysis of the western blot. Data are expressed as the means ± SE of three independent experiments and are expressed relative to a control. Results were statistically analyzed with Student's *t*-test ($^{*}P < 0.05$ and $^{**}P < 0.01$ compared with the TPA treatment only). (**D**) Cells were pretreated with the inhibitors at the indicated concentrations for 30 min and then stimulated with 200 nM TPA for 12 h. MMP-9 enzyme activities were determined by gelatin zymography as described in Materials and Methods.

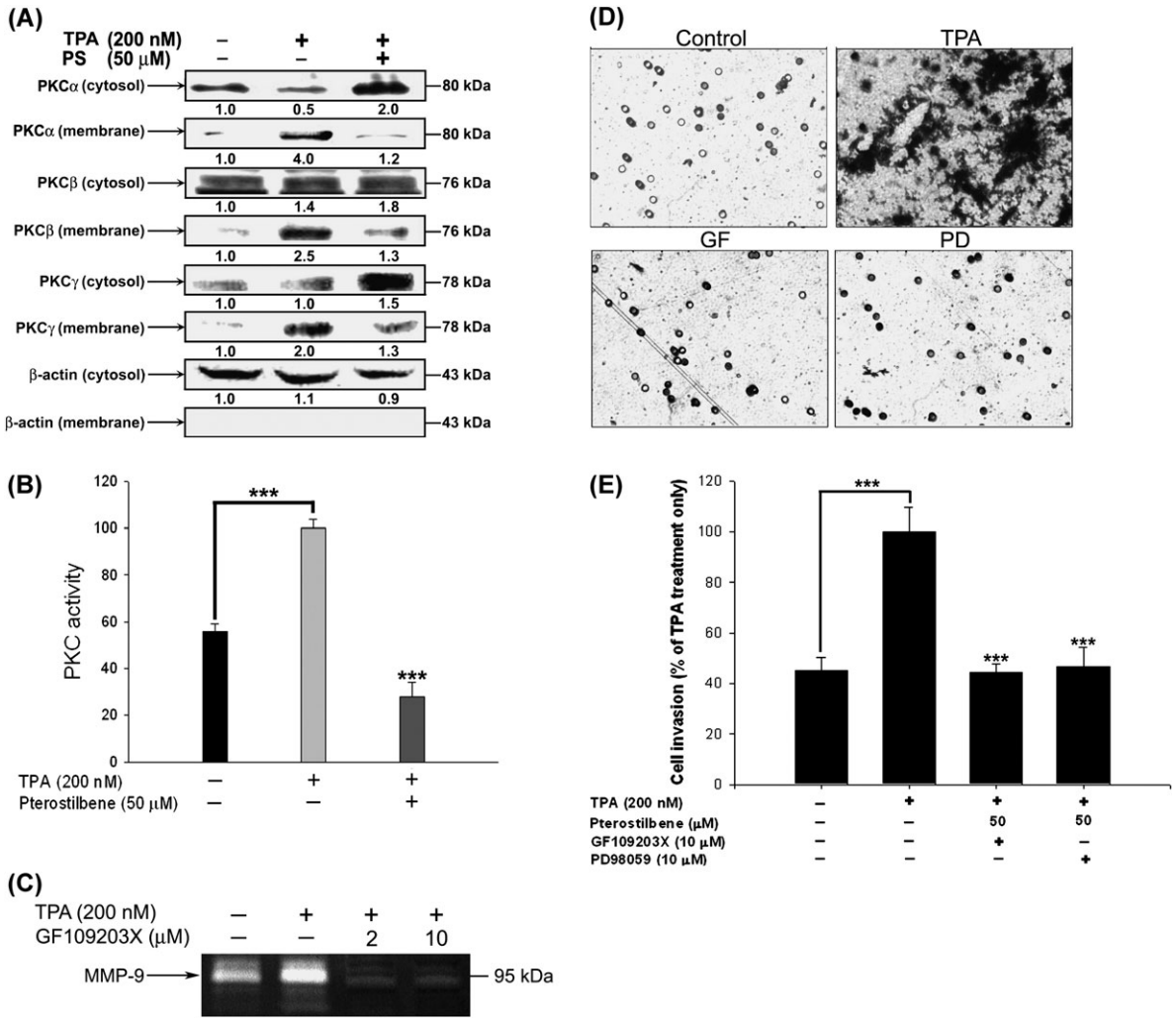

Fig. 6. Effects of pterostilbene (PS) on TPA-induced PKC activation (**A**) $HepG_2$ cells were cultured in serum-free media containing 200 nM TPA and 50 μM PS for 1.5 h, then the cell cytosolic and membrane fractions were prepared as described in Materials and Methods and then the extracts were analyzed by western blots as described in Materials and Methods. The values under each lane indicate relative density of the band normalized to β-actin. All analyses were representative of at least three independent experiments. (**B**) PKC activity was determined in the PKC kinase activity assay kit (non-radioactive) as described in Materials and Methods. Each bar represents the mean ± SE of the averages of triplicate experiments. Results were statistically analyzed with Student's *t*-test ($^{***}P < 0.001$ compared with the TPA treatment only). Cells were pretreated with the inhibitors at the indicated concentrations for 30 min and then stimulated with 200 nM TPA for 12 h (**C**) and incubated in the presence or absence of PS 50 μM for 24 h (D). (C) The gelatinolytic activities of MMP-9 were determined by gelatin zymography as described in Materials and Methods. (**D**) The invasion ability was examined by a Matrigel coated under the microscope in three random fields at a ×400 magnification. (**E**) Each bar represents the mean ± SE of the averages of triplicate plates and three fields counted. Results were statistically analyzed with Student's *t*-test ($^{***}P < 0.001$ compared with the TPA treatment only).

vein to imitate tumor metastasis. As shown in supplementary Figure 1A (available at *Carcinogenesis* Online), throughout the experiment, there was no noticeable difference in weight gain between the mice treated with two doses of pterostilbene and those not treated, indicating that the intraperitoneal administration of pterostilbene did not cause any toxicity. When pterostilbene was administrated, at a dose of 20 or 250 mg/kg, the average number of foci per mouse was markedly reduced by 56.8 and 63.8%, respectively (supplementary Figure 1B is available at *Carcinogenesis* Online). Furthermore, in mice receiving these treatment regimens, no gross signs of toxicity were observed (body weight, visible inspection of general appearance and microscopic examination of individual organs). We further investigated MMP-9 enzyme activity and VEGF level in the plasma of mice treated with pterostilbene. As shown in supplementary Figure 1C (available at *Carcinogenesis* Online), MMP-9 enzyme activities and VEGF levels were markedly inhibited in pterostilbene-treated mice. Our results provide further evidence that such observations may have significance for cancer chemotherapeutic purposes.

Discussion

Epidemiological studies link the consumption of fruits and vegetables to a reduced risk of several types of human cancer (33). Laboratory animal studies provide evidences that pterostilbene significantly suppressed azoxymethane-induced formation of aberrant crypt foci and multiple clusters of aberrant crypts and inhibited azoxymethane-induced inducible nitric oxide synthase expression (34). It is widely believed that misregulation of this pathway leads to the development of cancer. Reflecting this knowledge, the mechanism of action for many currently used anticancer agents is specifically targeted to regulate the apoptotic pathway, further stressing the role of programmed cell death in maintaining normal homeostasis. Research indicates that one of the mechanisms for some of these bioactives is through the signaling pathway inducing programmed cell death (35). Our recent study indicated that pterostilbene induced apoptosis in human gastric adenocarcinoma cell line cells through activating the caspase cascade via the mitochondrial and Fas/FasL pathway, growth arrest and DNA

damage expression and by modifying cell cycle progress and changes in several cell cycle-regulating protein (36). Although pterostilbene was reported to possess anti-metastatic potential against mouse B16 melanoma F10 cells (37), however, the role of pterostilbene against TPA-induced MMP-9 expression and invasiveness of human hepatoma cells is still unclear. Our previous study found that pterostilbene suppressed not only TPA-induced MMP-9 activity but also MMP-2 activity. The present study showed that pterostilbene effectively suppressed TPA-induced *MMP-9* gene expression via suppressing the PKCs/MAPK/AP-1 and PI3K/AKT/NF-κB cascades with consequent suppression of colony formation, tumor migration and invasion by human hepatoma $HepG_2$ cells.

Activation of NF-κB and AP-1 is centrally involved in the induction of the *MMP-9* gene associated with the invasion and metastasis of tumor cells by different agents including TPA, growth factors such as EGF, VEGF, platelet-derived growth factor, transforming growth factor-β and inflammatory cytokines (12,13). Thus, the regulation of NF-κB and AP-1, downstream of the PI3K/Akt and MAPK pathways, might be involved in pterostilbene suppressed TPA-induced MMP-9 expression and invasion in $HepG_2$ cells. Weng *et al.* (30) reported that TPA treatment for 24 h activates NF-κB and AP-1 with an increase in MMP-9 expression in human hepatoma cells. We demonstrated that luciferase activity of NF-κB and AP-1 is significantly increased by treatment with TPA, whereas these were blocked by pretreatment with pterostilbene (Figure 4).

Many signaling pathways, including PI3K/Akt, MAPK and PKC, are proposed to respond to TPA stimulation (38). PI3K activation leads to phosphorylation of phosphatidylinositides, which then activates the downstream main target, Akt, which appears to play various important roles in regulating cellular growth, differentiation, adhesion, the inflammatory reaction and invasion (21,39). Induction of MAPK (ERK1/2, p38 and JNK) and PI3K/Akt is involved in MMP-9 expression in different cell types (17,21); however, the signaling pathway related to MMP-9 expression evoked by TPA in $HepG_2$ cells is still unclear. Weng *et al.* (30) showed that lucidenic acid inhibits the transcription activity of MMP-9 in the TPA-induced $HepG_2$ cells by suppressing MAPK/ERK and inhibiting NF-κB and AP-1 DNA-binding activities. Chung *et al.* (40) reported that caffeic acid and caffeic acid phenethyl ester suppress the transcriptional activity of MMP-9 in TPA-induced $HepG_2$ cells by inhibiting NF-κB activation. Woo *et al.* (41) also found that resveratrol suppresses MMP-9 expression in TPA-induced human Caski cells by blocking JNK and PKCδ signal transduction. Since pterostilbene can significantly inhibit the induction of *MMP-9* genes and proteins, we investigated whether pterostilbene exerts any influence or interferes with signaling molecules, in turn regulating them. Our present study found that TPA can activate both MAPK and PI3K/Akt in $HepG_2$ cells, and these can be diminished by pterostilbene (Figure 5).

It is generally accepted that PKC is major cellular receptor for diacylglycerol and TPA, and it is thought that many of its tumor promotional, invasive, inflammatory and proliferative effects are mediated through the activation of one or more PKC isoform. Moreover, PKCs have also been implicated in the promotion and/or progression phase of carcinogenesis (42). In agreement with a study by Weng *et al.* (30), stimulation of PKC activation by TPA is critical for the induction of MMP-9 expression and invasiveness of hepatoma cells, and these were blocked by pterostilbene (Figure 6). Since the structure of pterostilbene is non-polar, it could be either lodged in a membrane and affect $HepG_2$ cell access to TPA uptake or directly inhibit membrane-bound PKC. We do not rule out a possible mechanism in which lipophilic pterostilbene penetrates cells and, probably, competes with coenzymes or adenosine triphosphate to inhibit the activity of PKC. Tumors and stimulators have been shown to induce MMP-9 expression in multiple biological functions such as extravasation, migration, survival in the microenvironment, angiogenesis and tumorigenicity (43). Further, thorough evaluation of the anti-metastatic potential of pterostilbene *in vivo*, we first demonstrated that pterostilbene reduced tumor metastasis in lung (supplementary Figure 1 is available at *Carcinogenesis* Online). In the pulmonary metastasis experiment, the plasma levels of pterostilbene at 30 min after intraperitoneal administration (50 and 250 mg/kg) were estimated to be 2.24 and 26.85 μg/ml, respectively. However, pterostilbene was detectable even 24 h after intraperitoneal administration. The plasma levels of pterostilbene were 0.05 and 0.39 μg/ml, respectively. Moreover, the animals were dosed intravenously with pterostilbene; the glucuronidated pterostilbene metabolite was detected in both serum and urine (1). According to our study, we suggested that pterostilbene at 50 μM is corresponding to ∼710 mg of daily administration in adult human being of 70 kg body wt.

Based on our finding, we suggest that pterostilbene promotes a strong protective effect against TPA-mediated metastasis via down-regulation of early and long-term inside-out signaling process. Together, as illustrated in supplementary Figure 2 (available at *Carcinogenesis* Online), our present study provides proof that, through a molecular mechanism, pterostilbene promotes a strong anti-invasive and anti-metastatic effect against TPA-mediated metastasis via down-regulation of PKC, EGF and VEGF then blocked MAPK- and PI3K/Akt-signaling pathways, NF-κB and AP-1 transcription factors, as well as MMP-9. Therefore, we conclude that MMP-9 inhibition activity of pterostilbene and its inhibition of multiple signal transduction pathways have a therapeutic potential, giving a novel means of controlling invasiveness and metastasis of tumors.

Supplementary material

Supplementary Figures 1–2 can be found at http://carcin.oxfordjournals.org/

Funding

National Science Council (NSC 95-2313-B-022-003-MY3, NSC 97-2321-B-022-001).

Acknowledgements

Conflict of Interest Statement: None declared.

References

1. Remsberg,C.M. *et al*. (2008) Pharmacometrics of pterostilbene: preclinical pharmacokinetics and metabolism, anticancer, antiinflammatory, antioxidant and analgesic activity. *Phytother. Res.*, **22**, 169–179.
2. Pan,M.H. *et al*. (2008) Pterostilbene suppressed lipopolysaccharide-induced up-expression of iNOS and COX-2 in murine macrophages. *J. Agric. Food Chem.*, **56**, 7502–7509.
3. Bergsland,E.K. *et al*. (2000) Hepatocellular carcinoma. *Curr. Opin. Oncol.*, **12**, 357–361.
4. Izumi,R. *et al*. (1994) Prognostic factors of hepatocellular carcinoma in patients undergoing hepatic resection. *Gastroenterology*, **106**, 720–727.
5. Kilian,M. *et al*. (2006) Matrix metalloproteinase inhibitor RO 28-2653 decreases liver metastasis by reduction of MMP-2 and MMP-9 concentration in BOP-induced ductal pancreatic cancer in Syrian Hamsters: inhibition of matrix metalloproteinases in pancreatic cancer. *Prostaglandins Leukot. Essent. Fatty Acids*, **75**, 429–434.
6. Mizutani,K. *et al*. (2000) The significance of MMP-1 and MMP-2 in peritoneal disseminated metastasis of gastric cancer. *Surg. Today*, **30**, 614–621.
7. Gullu,I.H. *et al*. (2000) The relation of gelatinase (MMP-2 and -9) expression with distant site metastasis and tumour aggressiveness in colorectal cancer. *Br. J. Cancer*, **82**, 249.
8. Yan,C. *et al*. (2007) Regulation of matrix metalloproteinase gene expression. *J. Cell. Physiol.*, **211**, 19–26.
9. Donadio,A.C. *et al*. (2008) Extracellular matrix metalloproteinase inducer (EMMPRIN) and matrix metalloproteinases (MMPs) as regulators of tumor-host interaction in a spontaneous metastasis model in rats. *Histochem. Cell Biol.*, **130**, 1155–1164.
10. Cortes-Reynosa,P. *et al*. (2008) Src kinase regulates metalloproteinase-9 secretion induced by type IV collagen in MCF-7 human breast cancer cells. *Matrix Biol.*, **27**, 220–231.

11. Okuducu,A.F. *et al*. (2006) Ets-1 is up-regulated together with its target gene products matrix metalloproteinase-2 and matrix metalloproteinase-9 in atypical and anaplastic meningiomas. *Histopathology*, **48**, 836–845.
12. Nee,L. *et al*. (2007) TNF-alpha and IL-1 beta-mediated regulation of MMP-9 and TIMP-1 in human glomerular mesangial cells. *Nephron. Exp. Nephrol.*, **107**, e73–e86.
13. Hollborn,M. *et al*. (2007) Positive feedback regulation between MMP-9 and VEGF in human RPE cells. *Invest. Ophthalmol. Vis. Sci.*, **48**, 4360–4367.
14. Cowden Dahl,K.D. *et al*. (2008) Matrix metalloproteinase 9 is a mediator of epidermal growth factor-dependent e-cadherin loss in ovarian carcinoma cells. *Cancer Res.*, **68**, 4606–4613.
15. Zeisberg,M. *et al*. (2002) Renal fibrosis. Extracellular matrix microenvironment regulates migratory behavior of activated tubular epithelial cells. *Am. J. Pathol.*, **160**, 2001–2008.
16. Lee,S.O. *et al*. (2008) Suppression of PMA-induced tumor cell invasion by capillarisin via the inhibition of NF-kappaB-dependent MMP-9 expression. *Biochem. Biophys. Res. Commun.*, **366**, 1019–1024.
17. Lee,S.O. *et al*. (2007) Silibinin suppresses PMA-induced MMP-9 expression by blocking the AP-1 activation via MAPK signaling pathways in MCF-7 human breast carcinoma cells. *Biochem. Biophys. Res. Commun.*, **354**, 165–171.
18. Cho,H.J. *et al*. (2007) Ascofuranone suppresses PMA-mediated matrix metalloproteinase-9 gene activation through the Ras/Raf/MEK/ERK- and Ap1-dependent mechanisms. *Carcinogenesis*, **28**, 1104–1110.
19. Griner,E.M. *et al*. (2007) Protein kinase C and other diacylglycerol effectors in cancer. *Nat. Rev. Cancer*, **7**, 281–294.
20. Zhang,S. *et al*. (2006) Methyl-3-indolylacetate inhibits cancer cell invasion by targeting the MEK1/2-ERK1/2 signaling pathway. *Mol. Cancer Ther.*, **5**, 3285–3293.
21. Chung,T.W. *et al*. (2004) Hepatitis B viral HBx induces matrix metalloproteinase-9 gene expression through activation of ERK and PI-3K/AKT pathways: involvement of invasive potential. *FASEB J.*, **18**, 1123–1125.
22. Chakraborti,S. *et al*. (2003) Regulation of matrix metalloproteinases: an overview. *Mol. Cell. Biochem.*, **253**, 269–285.
23. Simon,C. *et al*. (2001) The p38 SAPK pathway regulates the expression of the MMP-9 collagenase via AP-1-dependent promoter activation. *Exp. Cell Res.*, **271**, 344–355.
24. Guruvayoorappan,C. *et al*. (2008) Amentoflavone inhibits experimental tumor metastasis through a regulatory mechanism involving MMP-2, MMP-9, prolyl hydroxylase, lysyl oxidase, VEGF, ERK-1, ERK-2, STAT-1, nm23 and cytokines in lung tissues of C57BL/6 mice. *Immunopharmacol. Immunotoxicol.*, **30**, 711–727.
25. Waas,E.T. *et al*. (2003) Matrix metalloproteinase 2 and 9 activity in patients with colorectal cancer liver metastasis. *Br. J. Surg.*, **90**, 1556–1564.
26. Okada,N. *et al*. (2001) Matrix metalloproteinase-2 and -9 in bile as a marker of liver metastasis in colorectal cancer. *Biochem. Biophys. Res. Commun.*, **288**, 212–216.
27. Pettit,G.R. *et al*. (2002) Antineoplastic agents. 465. Structural modification of resveratrol: sodium resverastatin phosphate. *J. Med. Chem.*, **45**, 2534–2542.
28. George,S.E. *et al*. (1997) Functional coupling of endogenous serotonin (5-HT1B) and calcitonin (C1a) receptors in CHO cells to a cyclic AMP-responsive luciferase reporter gene. *J. Neurochem.*, **69**, 1278–1285.
29. Kajanne,R. *et al*. (2007) EGF-R regulates MMP function in fibroblasts through MAPK and AP-1 pathways. *J. Cell. Physiol.*, **212**, 489–497.
30. Weng,C.J. *et al*. (2008) Lucidenic acid inhibits PMA-induced invasion of human hepatoma cells through inactivating MAPK/ERK signal transduction pathway and reducing binding activities of NF-kappaB and AP-1. *Carcinogenesis*, **29**, 147–156.
31. Kikkawa,U. *et al*. (1983) Protein kinase C as a possible receptor protein of tumor-promoting phorbol esters. *J. Biol. Chem.*, **258**, 11442–11445.
32. Guo,K. *et al*. (2008) Role of PKCbeta in hepatocellular carcinoma cells migration and invasion *in vitro*: a potential therapeutic target. *Clin. Exp. Metastasis*, **26**, 189–195.
33. Pan,M.H. *et al*. (2008) Chemopreventive effects of natural dietary compounds on cancer development. *Chem. Soc. Rev.*, **37**, 2558–2574.
34. Suh,N. *et al*. (2007) Pterostilbene, an active constituent of blueberries, suppresses aberrant crypt foci formation in the azoxymethane-induced colon carcinogenesis model in rats. *Clin. Cancer Res.*, **13**, 350–355.
35. Pan,M.H. *et al*. (2008) Food bioactives, apoptosis, and cancer. *Mol. Nutr. Food Res.*, **52**, 43–52.
36. Pan,M.H. *et al*. (2007) Pterostilbene induces apoptosis and cell cycle arrest in human gastric carcinoma cells. *J. Agric. Food Chem.*, **55**, 7777–7785.
37. Ferrer,P. *et al*. (2005) Association between pterostilbene and quercetin inhibits metastatic activity of B16 melanoma. *Neoplasia*, **7**, 37–47.
38. Murayama,K. *et al*. (2007) Akt activation induces epidermal hyperplasia and proliferation of epidermal progenitors. *Oncogene*, **26**, 4882–4888.
39. Carpenter,C.L. *et al*. (1996) Phosphoinositide kinases. *Curr. Opin. Cell Biol.*, **8**, 153–158.
40. Chung,T.W. *et al*. (2004) Novel and therapeutic effect of caffeic acid and caffeic acid phenyl ester on hepatocarcinoma cells: complete regression of hepatoma growth and metastasis by dual mechanism. *FASEB J.*, **18**, 1670–1681.
41. Woo,J.H. *et al*. (2004) Resveratrol inhibits phorbol myristate acetate-induced matrix metalloproteinase-9 expression by inhibiting JNK and PKC delta signal transduction. *Oncogene*, **23**, 1845–1853.
42. Garg,R. *et al*. (2008) Curcumin decreases 12-O-tetradecanoylphorbol-13-acetate-induced protein kinase C translocation to modulate downstream targets in mouse skin. *Carcinogenesis*, **29**, 1249–1257.
43. Hunter,K.W. *et al*. (2008) Mechanisms of metastasis. *Breast Cancer Res.*, **10** (suppl. 1), S2.

Received March 2, 2009; revised May 8, 2009; accepted May 8, 2009